



# Probing non-enzymatic glycation of type I collagen: A novel approach using Raman and infrared biophotonic methods



Marie Guilbert<sup>a</sup>, Georges Said<sup>a</sup>, Teddy Happillon<sup>a</sup>, Valérie Untereiner<sup>a</sup>, Roselyne Garnotel<sup>a</sup>, Pierre Jeannesson<sup>a</sup>, Ganesh D. Sockalingum<sup>a,\*</sup>

<sup>a</sup> Equipe MEdIAN-Biophotonique et Technologies pour la Santé, Université de Reims Champagne-Ardenne, Unité MEDyC FRE CNRS/URCA 3481, UFR de Pharmacie, 51 rue Cognacq-Jay, 51096 Reims, France

## ARTICLE INFO

### Article history:

Received 9 October 2012  
Received in revised form 8 January 2013  
Accepted 13 January 2013  
Available online 1 February 2013

### Keywords:

Type I collagen  
Glycation  
Advanced Glycation End products  
Fourier-transform infrared microspectroscopy  
Raman microspectroscopy

## ABSTRACT

**Background:** Non-enzymatic glycation is the main post-translational modification of long-life proteins observed during aging and physiopathological processes such as diabetes and atherosclerosis. Type I collagen, the major component in matrices and tissues, represents a key target of this spontaneous reaction which leads to changes in collagen biomechanical properties and by this way to tissue damages.

**Methods:** The current study was performed on *in vitro* glycated type I collagens using vibrational microspectroscopies, FT-IR and Raman, to highlight spectral features related to glycation effect.

**Results and conclusions:** We report a conservation of the triple-helical structure of type I collagen and noticeable variations in the exposure of proline upon glycation. Our data also show that the carbohydrate band can be a good spectroscopic marker of the glycation level, correlating well with the fluorescent AGEs formation with sugar addition.

**General significance:** These non-invasive and label-free methods can shed new light on the spectral features of glycated collagens and represent an effective tool to study changes in the extracellular matrix observed *in vivo* during aging or on the advent of a pathological situation.

© 2013 Elsevier B.V. All rights reserved.

## 1. Introduction

Type I collagen is the most abundant extracellular matrix protein in the human body. It is assembled in triple-helical structure, and cross-linking between triple helices allows it to form a fibrillar network [1]. Because of its long lifespan which can be variable, about 15-years in skin, collagen I undergoes post-translational modifications during aging or pathological conditions such as diabetes mellitus [2] and more recently in cancer processes [3,4]. The main modification is a non-enzymatic glycation [5,6], resulting in the fixation of reducing agents, such as aldose sugars, essentially on lysine residues of type I collagen. In the field of cancer, scaffolds of glycated collagens have been used to study the impact of this post-translational modification on tumor cell proliferation [7] and migration [8]. Further, in tissue engineering strategies, glycated collagen has also been shown to be of great interest for preparing cartilage constructs [9,10], mimicking

diabetic wound healing [11] or evaluating the effect of mechanical constraints on cellular behavior [12].

At the mechanistic level, glycation leads to the formation of Schiff bases that are transformed into Amadori products. After complex rearrangements, the Amadori compounds give rise to irreversible products called advanced glycation end products (AGEs) [3]. Among these end products, N<sup>ε</sup>-carboxymethyllysine (CML) and pyrraline have been found to be non-fluorescent and non-cross-linking, while pentosidine and crossline have been described as fluorescent and cross-linking compounds [13–15]. AGEs contribute to changes in the collagen properties such as loss of the triple helix solubility and flexibility, resulting in an increase of its rigidity [1]. Consequently, *via* these structural and molecular modifications of collagen triple helix, its enzymatic digestibility is less efficient with aging and in pathological situations like diabetes [16]. Glucose is the major blood circulating sugar in the human body but it exhibits less reducing properties than agents such as ribose, glyceraldehydes or fructose [4,17]. Although these latter compounds are less involved in *in vivo* protein glycation processes, they are able to generate elevated AGEs levels and are therefore used for *in vitro* collagen glycation [1].

Protein glycation evaluation is currently assessed by conventional spectrometric, chromatographic or immunohistochemical methods. To detect post-translational modifications of the collagen and to provide a quantitative determination of resulting cross-links, mass spectrometry and high performance liquid chromatography have

\* Corresponding author at: FRE CNRS/URCA no. 3481, UFR Pharmacie, 51 rue Cognacq-Jay, 51096 Reims Cedex, France. Tel.: +33 3 26 91 35 53; fax: +33 3 26 91 35 50.

E-mail addresses: [marie.guilbert@univ-reims.fr](mailto:marie.guilbert@univ-reims.fr) (M. Guilbert), [georgessaid@gmail.com](mailto:georgessaid@gmail.com) (G. Said), [teddy.happillon@gmail.com](mailto:teddy.happillon@gmail.com) (T. Happillon), [valerie.untreiner@univ-reims.fr](mailto:valerie.untreiner@univ-reims.fr) (V. Untereiner), [roselyne.garnotel@univ-reims.fr](mailto:roselyne.garnotel@univ-reims.fr) (R. Garnotel), [pierre.jeannesson@univ-reims.fr](mailto:pierre.jeannesson@univ-reims.fr) (P. Jeannesson), [ganesh.sockalingum@univ-reims.fr](mailto:ganesh.sockalingum@univ-reims.fr) (G.D. Sockalingum).

been largely used [14,16]. However, these methods need sample reduction and protein hydrolysis into amino-acids [18] and as such cannot be used directly on *ex vivo* or *in vivo* tissues. For immunostaining of tissues, AGEs' accumulation can be also quantified but it gives the AGEs' content from all proteins present in the tissue section, but not from a single protein like collagen [19,20]. For these reasons, the most current technique used to quantify glycation rate of collagen is the fluorimetric assay that permits to detect fluorescent AGEs such as pentosidine [21]. However, even if this technique provides AGEs' quantification, it does not inform on the molecular changes associated to the overall AGEs.

In the present study, we investigated the non-enzymatic glycation process of type I collagen using a biophotonic complementary approach based on infrared and Raman vibrational microspectroscopies. These robust and non-invasive methods can provide information on both the composition and the structure, and are sensitive to the environment of proteins [22,23]. They are well adapted to highlight the impact of non-enzymatic glycation directly on type I collagen. In particular, Roy *et al.* [24] have previously demonstrated that Fourier-transform infrared (FT-IR) used in the Attenuated Total Reflection (ATR) mode allowed to quantify *in vitro* glycation of collagen gels, which was clearly correlated with the fluorescent-AGEs' accumulation. In our study, in addition to the FT-IR microspectroscopic approach, we have used Raman microspectroscopy to complement the analysis of native, fibrillar, and non-pepsined type I collagen *in vitro*-glycated with glucose or ribose. These vibrational spectroscopic techniques are label-free, direct, rapid, and non-destructive approaches that are applied here to explore to what extent *in vitro* glycation of type I collagen impact on protein structural features. Both methodologies are sensitive to molecular and conformational structural information and are complementary.

## 2. Material and methods

### 2.1. Extraction of type I collagen and *in vitro* glycation

Fibrillar type I collagen was extracted as previously described [25]. Briefly, acid-soluble type I collagen was obtained from tail tendons of Sprague-Dawley rats by 0.5 M acetic acid extraction then purified by dialysis against distilled water and lyophilized. This native, purified, and non-pepsined collagen was stored at  $-80^{\circ}\text{C}$  until further use. For preparation of *in vitro* glycated collagens, the lyophilized extracted native type I collagen was incubated, under sterile conditions, at  $37^{\circ}\text{C}$  for 14 days in 0.15 M of phosphate buffer pH 7.4 containing 5 or 50 mM of glucose (Sigma-Aldrich, L'isle d'Abeau Chesnes, France) or for 5 days in the same buffer containing 50 mM of ribose (Sigma-Aldrich). Both types of glycated collagens were extensively dialyzed against distilled water and then lyophilized.

### 2.2. Estimation of electrophoretic properties

Collagens were solubilized at 2 mg/ml in 0.018 M of acetic acid (v/v) and denatured by heating for 2 min at  $90^{\circ}\text{C}$ . Electrophoretic properties of native and *in vitro*-glycated collagens were estimated by 5% sodium dodecyl sulfate-polyacrylamide gel electrophoresis (SDS-PAGE). Gels were stained with Coomassie Brilliant Blue R250 for revealing characteristic type I collagen chains.

### 2.3. Fluorescent AGEs detection

To quantify the glycation level in the *in vitro*-glycated collagens, AGEs-specific fluorescence was measured using a Shimadzu RF-5000 fluorescence spectrophotometer (Shimadzu, Marne la Vallée, France) at 380 nm excitation and 440 nm emission, after solubilizing collagens at 2 mg/ml in 0.018 M of acetic acid (v/v). Data are presented as

mean  $\pm$  SEM. The values were analyzed with Kruskal–Wallis followed by Mann–Whitney tests. Statistical significance was set at  $p < 0.05$ .

### 2.4. FT-IR microspectroscopy

Micro-FT-IR acquisitions of lyophilized native and *in vitro*-glycated type I collagens were performed on thin pellets, prepared by mixing 1 mg of collagen with 99 mg of potassium bromide (Sigma-Aldrich) and pressed in the form of thin discs at 10,000–15,000 psi during 10 min. Infrared transmission spectra were recorded between 4000 and  $700\text{ cm}^{-1}$  in the point mode using a  $100 \times 100\text{ }\mu\text{m}^2$  aperture with a Spotlight 300 microscope coupled to a Spectrum 100 FT-IR spectrometer (both from Perkin Elmer, Courtaboeuf, France). For each spectrum, 128 scans were averaged at  $4\text{ cm}^{-1}$  resolution and data were pre-processed by baseline correction with the elastic correction method, vector normalized on the total spectral range, and offset corrected to bring the minimum absorbance value to 0, using the Opus 6.5 software (Bruker Optics, Marne la Vallée, France).

### 2.5. Raman microspectroscopy

Micro-Raman spectra were recorded directly on lyophilized native and *in vitro*-glycated type I collagens without further preparation using a Labram microspectrometer (Horiba Jobin-Yvon SAS, Lille, France) operating with a 785 nm diode laser (Spectra-Physics, Les Ulis, France) and equipped with a  $100 \times$  long working distance objective (numerical aperture of 0.8). For each measurement, two acquisitions of 80 s were averaged at  $4\text{ cm}^{-1}$  spectral resolution over the spectral window 350 to  $1800\text{ cm}^{-1}$ . All spectra were pre-processed by smoothing when necessary (7 points Savitzky–Golay smoothing), and then baseline corrected, vector normalized, and offset corrected, using the LabSpec 4.18 software (Horiba Jobin-Yvon).

### 2.6. Spectral data processing

Spectral data were compared using Hierarchical Clustering Analysis (HCA) that allows regrouping spectra on a minimal distance criterion and so, according to their homogeneity. For this purpose, Euclidian distances and Ward's algorithm implemented in the Opus 6.5 software (Bruker Optics) were used and the results were displayed via a dendrogram.

## 3. Results

### 3.1. Evaluation of *in vitro* glycation efficiency of type I collagen: electrophoretic mobility and fluorescent AGEs accumulation

In order to validate the accumulation of AGEs, we investigated the electrophoretic mobility of *in vitro*-glycated collagens and the fluorescence intensity associated with AGEs production after incubation of extracted type I collagen with glucose (5 or 50 mM) or ribose (50 mM). As shown in Fig. 1A, all *in vitro*-glycated collagens exhibit characteristic bands of native type I collagen, showing  $\alpha_1$  and  $\alpha_2$  chains. However, a decrease of the electrophoretic mobility can be observed in glycated collagens compared to the native one. This effect is more marked with ribose-glycated collagen, confirming the higher reducing effect of ribose on collagen I compared to glucose. Fig. 1B displays the results of spectrofluorimetric assay of non-glycated and *in vitro*-glycated type I collagens. A proportional increase in the fluorescence of collagens as a function of glycation level can be observed, indicating that the content of fluorescent AGEs increases with the concentration and nature of the reducing sugar. For instance, a two-fold increase of AGEs accumulation is observed in 50 mM ribose-glycated collagen compared to 50 mM glucose-glycated collagen, confirming the higher reducing effect of ribose.

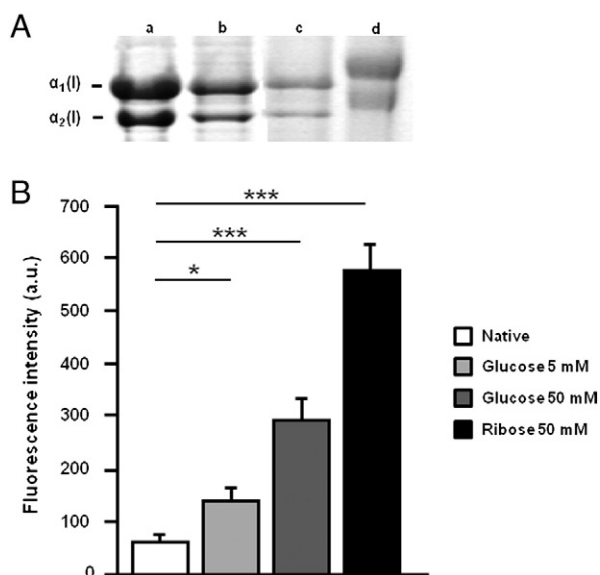


**Fig. 1.** Biochemical properties of *in vitro*-glycated collagens. (A) SDS-PAGE of collagen samples, 25  $\mu$ g of either native non-glycated (a) or *in vitro* glycated 5 mM glucose (b), 50 mM glucose (c), and 50 mM ribose (d) type I collagens were analyzed on 5% polyacrylamide gels under reducing conditions. (B) Spectrofluorimetric analysis was performed on these different collagens solubilized at 2 mg/ml in 18 mM acetic acid (v/v) to detect AGEs-specific fluorescence using a spectrofluorimeter (Shimadzu model RF-5000, France) at  $\lambda_{\text{ex}} = 380$  nm and  $\lambda_{\text{em}} = 440$  nm. Values are the mean of three independent experiments (\* $p < 0.05$  and \*\*\* $p < 0.001$  are compared to native non-glycated collagen, mean  $\pm$  SEM).

These two experimental results confirm the efficiency of the *in vitro* glycation process used in this study.

### 3.2. FT-IR microspectroscopic analysis of *in vitro* glycated collagens

Table 1 summarizes the FT-IR frequency positions and a tentative assignment of the major functional groups of native type I collagen with the changes observed with *in vitro* glycation in the characteristic peaks. It can be observed that the mean FT-IR spectrum of native non-glycated type I collagen exhibits the characteristic spectral features previously reported [26]. Comparison of the mean FT-IR spectra of *in vitro* glycated collagens with the control (Fig. 2) shows no significant change in the position of the Amide I band, representative of the protein secondary structure. This indicates that the triple helix structure of the molecule is well-conserved upon glycation. The up-shift observed in the Amide II band ( $1552 \text{ cm}^{-1}$  to  $1546 \text{ cm}^{-1}$ )

for ribose-glycated sample may reflect discrete conformational changes in tertiary structure of collagen such as changes of amino-acid exposure. Upon glycation, the most important changes are observed in the  $1100\text{--}900 \text{ cm}^{-1}$  spectral range, which corresponds to the characteristic absorption region of carbohydrates. In the native type I collagen, two distinct peaks are observed corresponding to total protein and carbohydrate signals ( $1082$  and  $1032 \text{ cm}^{-1}$  respectively). The signal of carbohydrates increases further until it becomes predominant over the total protein signal. In order to verify if these spectral modifications observed in this region can be a pertinent spectroscopic marker of the glycation degree, we have computed the intensity ratio of the  $1032 \text{ cm}^{-1}$  band with respect to the Amide I band at  $1660 \text{ cm}^{-1}$ . Our results clearly show that the  $I_{1030}/I_{1660}$  ratio increases (Fig. 3) of the same order as that observed for AGEs' detection by spectrofluorimetry.

An FT-IR spectrum contains at least a thousand of variables and another way of comparing spectral data is to use multivariate statistical analysis. Here, for instance, we applied HCA based on Ward's algorithm and Euclidean distance calculation, to determine spectral similarity via a plot of the heterogeneity values between spectra. The HCA of mean infrared spectra of native and glycated collagens using the total spectral range is displayed in Fig. 4A. As can be seen, it shows a clear discrimination between native and glycated collagens. For glycated samples, collagens are clearly differentiated as a function of the reducing sugar or the concentration used. The HCA performed on the carbohydrate region (Fig. 4B) confirms a clear-cut discrimination of the different collagens.

### 3.3. Raman microspectroscopic analysis of *in vitro* glycated collagens

In a complementary way, samples were also analyzed by Raman microspectroscopy in order to study molecular groups which may be active in Raman but not in FT-IR or active in both. The rationale is that while FT-IR spectra give information on the Amide I, corresponding to the stretching coordinate of  $\text{C}=\text{O}$  bonds ( $\nu\text{C}=\text{O}$ ) and Amide II corresponding to the deformation coordinate of  $\text{NH}_2$  groups ( $\delta\text{NH}_2$ ) bands Raman spectra exhibit Amide I ( $\nu\text{C}=\text{O}$ ) and Amide III ( $\delta\text{NH}_2$ ) features as well as side chain amino-acids.

The Raman mean spectra of both native type I collagen and *in vitro* glycated forms, shown in Fig. 5, exhibit the characteristic spectral features previously reported [27]. Spectra show that *in vitro* glycation does not alter the band positions of all functional groups since no frequency shift is observed. The Amide I ( $1673 \text{ cm}^{-1}$ ) and Amide III ( $1244 \text{ cm}^{-1}$ ) bands do not exhibit change, confirming the conservation of the triple-helix structure with *in vitro* glycation as yet demonstrated with FT-IR data. However, at the  $533 \text{ cm}^{-1}$  frequency position, it appears that the intensity of this Raman band increases upon glycation, suggesting conformational changes such as a skeletal deformation which may be due to the presence of cross-linking. Furthermore, other important changes in peak intensities are revealed upon glycation, especially for residues of prolines (Pro) and hydroxyprolines (HyPro) which are respectively the second and the third amino-acids in the type I collagen triple-helix composition. For each peak of interest, the ratio intensities ( $I_{\text{peak of interest}}/I_{1451}$ ) were calculated, the peak at  $1451 \text{ cm}^{-1}$  (assigned to  $-\text{CH}_2$  groups) remaining highly constant upon glycation. The observed changes are represented in Fig. 6, showing an increase of both the  $394 \text{ cm}^{-1}$  (HyPro) and  $875 \text{ cm}^{-1}$  (HyPro) peaks and a decrease of both the  $470 \text{ cm}^{-1}$  (Pro) and  $1556 \text{ cm}^{-1}$  (HyPro/Pro) peaks with glycation. These data suggest changes in the amino-acid exposure and protein backbone with type I collagen glycation. An HCA of Raman mean spectra (Fig. 7) using the total spectral range ( $350\text{--}1800 \text{ cm}^{-1}$ ) confirms a clear separation of glycated type I collagens from the native one and also a good discrimination as a function of the sugar or concentration used for *in vitro* glycation conditions.

**Table 1**  
Changes in vibrational band frequencies ( $\text{cm}^{-1}$ ) of characteristic FT-IR bands due to *in vitro* glycation of type I collagen.

|                                     | Native<br>(control) | Glucose<br>5 mM | Glucose<br>50 mM | Ribose<br>50 mM |
|-------------------------------------|---------------------|-----------------|------------------|-----------------|
| $\nu\text{NH}$                      | 3326                | 3326            | 3326             | 3326            |
| $\nu\text{NH}$                      | 3084                | 3084            | 3083             | 3083            |
| $\nu\text{CH}_2$                    | 2955                | 2955            | 2955             | 2955            |
| $\nu\text{CH}_2$                    | 2880                | 2880            | 2880             | 2880            |
| Amide I, $\nu\text{C}=\text{O}$     | 1660                | 1660            | 1660             | 1661            |
| Amide II, $\delta\text{NH}_2$       | 1552                | 1551            | 1550             | 1546            |
| $\delta\text{CH}_2$                 | 1453                | 1453            | 1452             | 1451            |
| $\delta\text{CH}_2$ , $\text{CH}_3$ | 1403                | 1403            | 1403             | 1403            |
| $\delta\text{CH}_2$                 | 1338                | 1338            | 1338             | 1338            |
| Amide III, $\delta\text{NH}_2$      | 1240                | 1240            | 1239             | 1237            |
| C–N                                 | 1205                | 1205            | 1205             | 1205            |
| C–OH                                | 1082                | 1082            | 1082             | 1082            |
| C–OH                                | 1032                | 1032            | 1032             | 1032            |

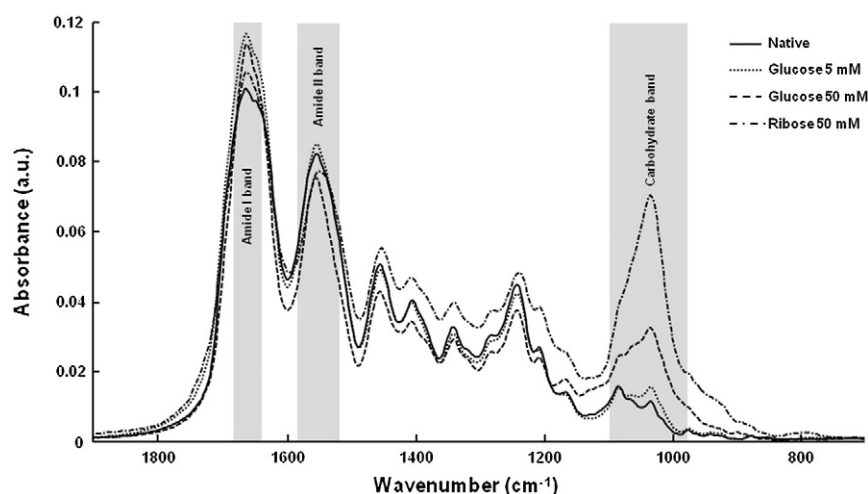


**Fig. 2.** FT-IR analysis of *in vitro*-glycated collagens. Comparison between FT-IR spectra of native non-glycated and *in vitro*-glycated (glucose 5 mM, glucose 50 mM and ribose 50 mM) collagens. Spectra represent means of three independent measurements and were normalized in the 1900–700  $\text{cm}^{-1}$  range. Gray zones indicate interest spectral regions to discriminate samples according to *in vitro* glycation.

#### 4. Discussion

In this study, IR and Raman microspectroscopies have been applied as probing non-destructive biophotonic techniques for studying native and glycated type I collagens. Results obtained demonstrate that upon *in vitro* glycation i) the conservation of the triple-helical structure of type I collagen; ii) noticeable variations in the exposure of proline, the second mostly abundant amino-acid in type I collagen chains; and iii) the level of glycation can be appreciated in a semi-quantitative manner. Concerning the third point, our results obtained at the microspectroscopic level largely confirm the previous observations highlighted by Roy et al. [24] using ATR-FTIR showing a direct proportionality between glycation level *via* the carbohydrate signal increase and the fluorescent-AGEs' formation.

This spectral analysis of non-enzymatic glycation is highly representative of the physiopathological range of glycation which impacts type I collagen *in vivo*. Indeed, the glucose concentrations used here are representative of the sugar content in mammalian circulating blood (5 mM) [28] and in severe diabetes (50 mM) [29,30]. In this pathology, it has been demonstrated that high glucose level leads to the formation of AGEs on proteins such as collagen or hemoglobin [31,32]. In this study, ribose being the highest reducing sugar, it permits a faster and higher glycation process compared to glucose. Even if it is not a physiological sugar, because of its higher reducing effect, it has been used for convenience reasons to glycate faster and therefore represents a positive control of protein glycation *in vitro* [16].

In this spectroscopic study, spectra of native and *in vitro* glycated type I collagens were recorded from thin pellets of the freeze-dried

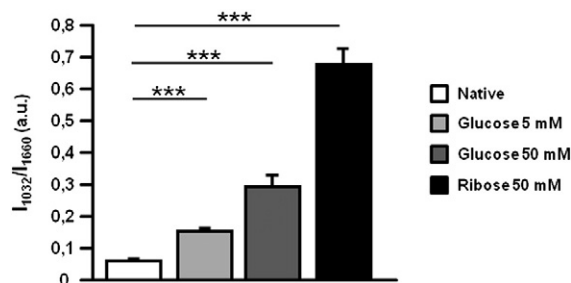


**Fig. 3.** Ratio of the FT-IR intensities ( $I$ ) of the carbohydrate and Amide I bands. The 1032  $\text{cm}^{-1}$  and 1660  $\text{cm}^{-1}$  peaks correspond at the FT-IR signal of C–OH bonds specific to carbohydrates and the FT-IR signal of Amide I band respectively. The ratio of the intensities of these two peaks ( $I_{1032}/I_{1660}$ ) was calculated.

proteins. The rationale for using freeze-dried form is that this procedure concentrates the proteins and provides well-resolved data for the spectroscopic analysis. Indeed, we have previously analyzed the native and *in vitro* glycated collagens in solution, but spectra were less informative compared to spectra from freeze-dried collagens since they exhibited only the Amide I band (data not shown). Furthermore, FT-IR spectra on the same solutions were completely dominated by water bands. Thus, the approach on freeze-dried collagens allows a comparative study in both infrared and Raman microspectroscopies,

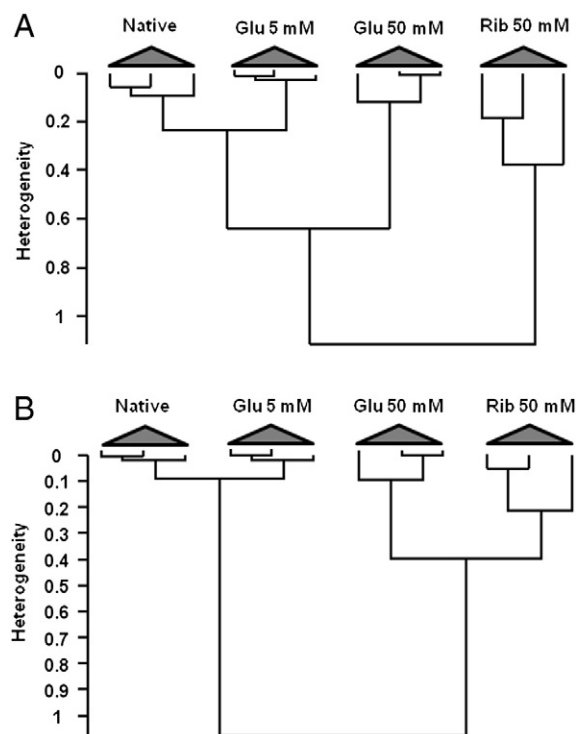


**Fig. 4.** Hierarchical cluster analysis (HCA) on FT-IR spectra from native and *in vitro*-glycated collagens. HCA was calculated with the mean spectra of three independent experiments for each condition, on the 4000–700  $\text{cm}^{-1}$  total spectral range (A) and on the spectral window 1100 to 900  $\text{cm}^{-1}$  corresponding to the specific fingerprint of carbohydrates (B). All mean spectra with a high homogeneity degree are clustered together.



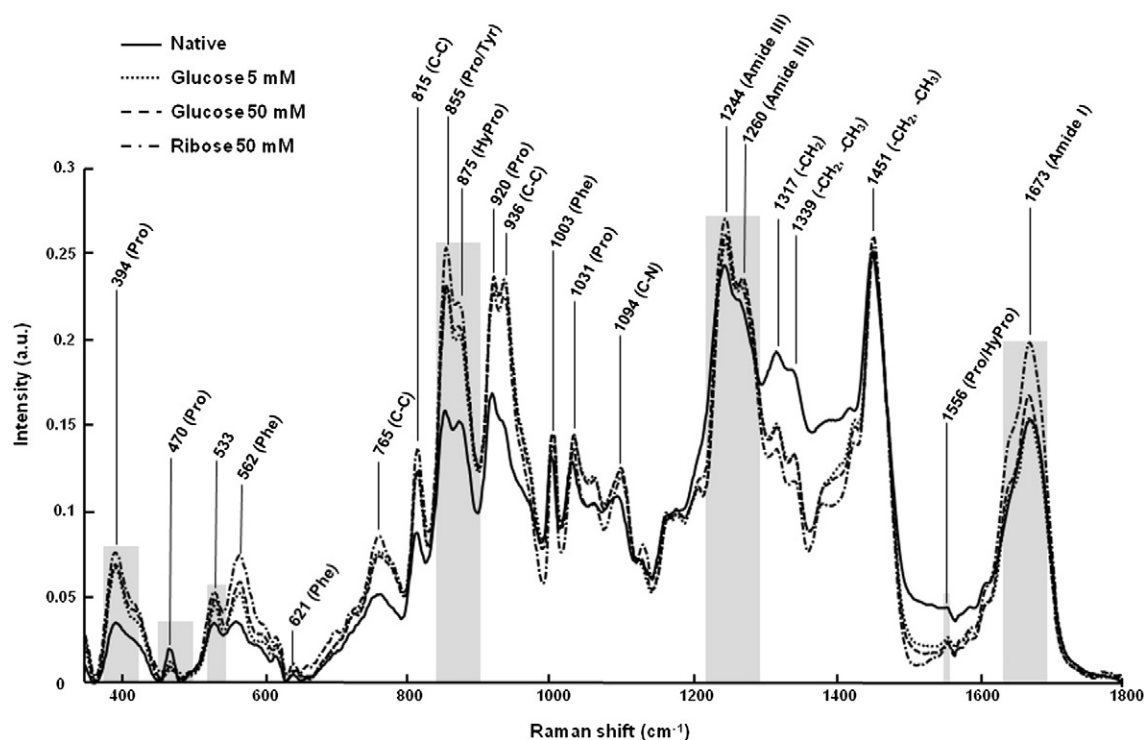


**Fig. 5.** Raman spectral analysis of *in vitro*-glycated collagens. Comparison between Raman spectra of native non-glycated and *in vitro*-glycated (glucose 5 mM, glucose 50 mM and ribose 50 mM) collagens. Spectra represent means of three independent measurements and were normalized in the 350–1800  $\text{cm}^{-1}$  range. Gray zones indicate interest spectral regions to discriminate samples according to *in vitro* glycation.

allowing the detection of minor spectral changes that occur upon *in vitro* glycation. In addition, it has been demonstrated by another biophotonic approach using pulsed terahertz spectroscopy, that the freeze-dried form is representative of proteins close to the hydrated form in terms of signal and can be considered as native protein [33].

In molecules with different elements of symmetry (such as in the triple-helical structure of collagen), certain bands may be active in IR, Raman, both or neither. That is why Raman and FT-IR microspectroscopies are complementary in the analysis of complex proteins such as collagen. In order to obtain a full vibrational fingerprint, samples

were analyzed by both FT-IR and Raman microspectroscopies. For example, in macromolecules or complex biomolecular systems, FT-IR gives a very high signal of carbohydrates, which is less discernable on a Raman spectrum. In contrast, the Raman spectrum of proteins better highlights amino-acid signatures and reveals the characteristic peaks of prolines and hydroxyprolines. These two residues are among the most important amino-acids present in the composition of both  $\alpha_1$  and  $\alpha_2$  chains of human collagens. Indeed, proline and hydroxyproline residues represent respectively the second (10%) and the third (8%) most abundant amino-acids in the protein sequence of type I collagen [34]. Their Raman activities exhibit important intensity differences between the native non-glycated (control) and glucose-glycated collagens and to a lesser extent for the ribose-glycated counterpart. These spectral modifications suggest that upon *in vitro* glycation, the molecule undergoes a slight supra-molecular rearrangement, resulting in variations

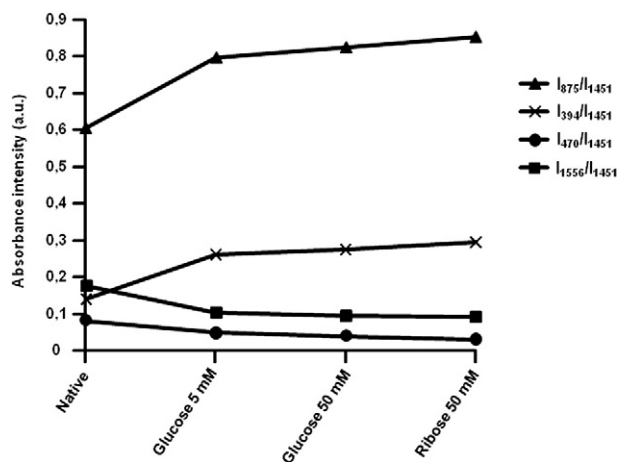


**Fig. 6.** Analysis of Raman signals from proline and hydroxyproline residues from native and *in vitro*-glycated collagens. The 1451  $\text{cm}^{-1}$  peak corresponds to the Raman signal of  $-\text{CH}_2$  and  $-\text{CH}_3$  groups, the 470  $\text{cm}^{-1}$  peak corresponds to the main Raman signal of prolines, the 394  $\text{cm}^{-1}$  and the 875  $\text{cm}^{-1}$  peaks correspond to the main Raman signal of hydroxyprolines, and the 1556  $\text{cm}^{-1}$  peak corresponds to the Raman signal of both prolines and hydroxyprolines. The ratio of the intensities of each of these peaks ( $I_{394}/I_{1451}$ ;  $I_{470}/I_{1451}$ ;  $I_{875}/I_{1451}$  and  $I_{1556}/I_{1451}$ ) was calculated.

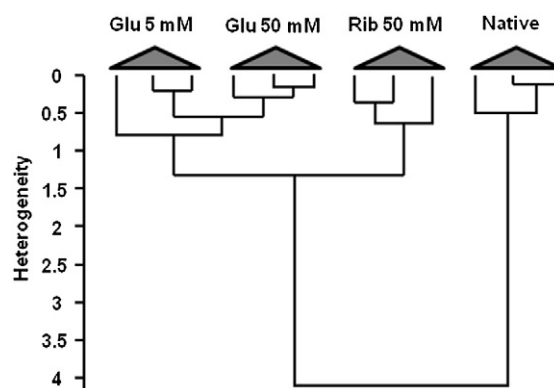


**Fig. 7.** Hierarchical cluster analysis (HCA) on Raman spectra from native and *in vitro*-glycated collagens. HCA was calculated with the mean spectra of three independent experiments for each condition, on the total spectral range (350–1800  $\text{cm}^{-1}$ ). All mean spectra with a high homogeneity degree are clustered together.

in the proline and hydroxyproline residue exposures. These observations, that can be associated with the increased AGEs formation induced by the glycation process, corroborate with the up-shift in the IR Amide II band, especially for ribose. The profiles of both the IR and Raman Amide I bands, well identified as representative of the secondary structure of proteins, exhibit neither intensity change nor band shift upon glucose or ribose exposure. This indicates that the triple-helical structure of type I collagen is not perturbed by the *in vitro* glycation. A recent study has confirmed similar observations with fructose, another reducing sugar, using circular dichroism and X-ray diffraction [35].

By integrating the area of the carbohydrate band ( $1100\text{--}900\text{ cm}^{-1}$ ), a semi-quantitative appreciation of the glycation level was possible. This spectral region therefore appears like a good IR spectroscopic marker of collagen I *in vitro* glycation. Recently, Roy et al. [24] have identified this spectral zone to characterize glycation levels between pre-glycated and post-glycated collagen gels. Further, we show that this spectroscopic marker is well correlated with the fluorescent-AGEs' quantification by conventional spectrofluorimetric assay. In parallel, at the tissue level, we recently reported that the intensity variations of this marker band can be highly indicative of changes in carbohydrate contents in glycoproteins such as human secreted mucins [36].

This study demonstrates the potential of vibrational microspectroscopies for detecting changes due to post-translational modifications of proteins. In addition, FT-IR and Raman microspectroscopies are rapid, sensitive, non-destructive and straight-forward techniques for analyzing sample composition and structure of proteins [37]. These biophotonic approaches are under constant progress for developing innovative tools for biomaterial molecular characterization. They are robust and well appropriate for evaluating structural changes in proteins and can be alternative and complementary tools to conventional techniques. In physiopathological conditions such as aging or diabetes, a major foreseen interest could be the direct evaluation of collagen glycation in tissues, as a complement to classical immunohistological detection assays.

## 5. Conclusions

The present study demonstrates that vibrational microspectroscopies allow detecting the effects of *in vitro* glycation on type I collagen, the major component in human tissues. We compared native type I collagen and *in vitro* glycated forms using reducing sugars and this model helped to highlight spectroscopic markers related to changes in the molecule upon glycation. Used in a complementary manner, FT-IR and Raman techniques can provide characteristic and specific spectral information of this non-enzymatic reaction. The spectral assignment for the triple-helical structure, that remained unchanged upon glycation, the proline and hydroxyproline attributions, and the carbohydrate band, which appear like a robust marker for a semi-quantitative appreciation of the glycation effect, are all very informative spectral ranges for studying post-translational modifications of matrix proteins. These techniques could be powerful tools for monitoring collagen changes occurring during aging or during the advent of pathological situations such as diabetes in a rapid, direct, quantitative, and label-free manner.

## Acknowledgements

This study was supported by grants of the Institut National du Cancer (INCa), the Cancéropôle Grand-Est and FEDER/CPER. M.G. is a recipient of a doctoral fellowship from Région Champagne-Ardenne and G.S. from Cancéropôle Grand-Est. We are thankful to Pr Hamid Morjani for his kind assistance with the spectrofluorimetric analysis. We thank the Plateforme IBiSA "Imagerie Cellulaire et Tissulaire" for providing the equipments.

## References

- [1] N.C. Avery, A.J. Bailey, The effects of the Maillard reaction on the physical properties and cell interactions of collagen, *Pathol. Biol.* 54 (2006) 387–395.
- [2] D.G. Dyer, J.A. Dunn, K.E. Bailie, T.J. Lyons, D.R. McCance, J.W. Baynes, Accumulation of Maillard reaction products in skin collagen in diabetes and aging, *J. Clin. Invest.* 91 (1993) 2463–2469.
- [3] N.A. Ansari, Z. Rasheed, Non-enzymatic glycation of proteins: from diabetes to cancer, *Biomed. Chim.* 56 (2010) 168–178.
- [4] J. Takino, S. Yamagishi, M. Takeuchi, Cancer malignancy is enhanced by glycerinaldehyde-derived advanced glycation end-products, *J. Oncol.* (2010) 739852.
- [5] R.G. Paul, A.J. Bailey, Glycation of collagen: the basis of its central role in the late complications of ageing and diabetes, *Int. J. Biochem. Cell Biol.* 28 (1996) 1297–1310.
- [6] M.E. Francis-Sedlak, S. Uriel, J.C. Larson, H.P. Greisler, D.C. Venerus, E.M. Brey, Characterization of type I collagen gels modified by glycation, *Biomaterials* 30 (2009) 1851–1856.
- [7] B. Bartling, M. Desole, S. Rohrbach, R.E. Silber, A. Simm, Age-associated changes of extracellular matrix collagen impair lung cancer cell migration, *FASEB J.* 23 (2009) 1510–1520.
- [8] G. Said, M. Guilbert, E. Millerot-Serruot, L. Van Gulick, C. Terryn, R. Garnotel, P. Jeannesson, Impact of carbamylation and glycation of collagen type I on migration of HT1080 human fibrosarcoma cells, *Int. J. Oncol.* 40 (2012) 1797–1804.
- [9] R. Roy, A.L. Boskey, L.J. Bonassar, Non-enzymatic glycation of chondrocyte-seeded collagen gels for cartilage tissue engineering, *J. Orthop. Res.* 26 (2008) 1434–1439.
- [10] S.V. Eleswarapu, J.A. Chen, K.A. Athanasios, Temporal assessment of ribose treatment on self-assembled articular cartilage constructs, *Biochem. Biophys. Res. Commun.* 414 (2011) 431–436.
- [11] H. Liao, J. Zakhaleva, W. Chen, Cells and tissue interactions with glycated collagen and their relevance to delayed diabetic wound healing, *Biomaterials* 30 (2009) 1689–1696.
- [12] B.N. Mason, A. Starchenko, R.M. Williams, L.J. Bonassar, C.A. Reinhart-King, Tuning three-dimensional collagen matrix stiffness independently of collagen concentration modulates endothelial cell behavior, *Acta Biomater.* 9 (2013) 4635–4644.
- [13] N. Ahmed, Advanced glycation endproducts—role in pathology of diabetic complications, *Diabetes Res. Clin. Pract.* 67 (2005) 3–21.
- [14] K. Mikulíková, A. Eckhardt, S. Pataridis, I. Miksik, Study of posttranslational non-enzymatic modifications of collagen using capillary electrophoresis/mass spectrometry and high performance liquid chromatography/mass spectrometry, *J. Chromatogr. A* 1155 (2007) 125–133.
- [15] F.J. Tessier, The Maillard reaction in the human body. The main discoveries and factors that affect glycation, *Pathol. Biol.* 58 (2010) 214–219.
- [16] S.F. Tian, S. Toda, H. Higashino, S. Matsumura, Glycation decreases the stability of the triple-helical strands of fibrous collagen against proteolytic degradation by pepsin in a specific temperature range, *J. Biochem.* 120 (1996) 1153–1162.
- [17] M.J. Kent, N.D. Light, A.J. Bailey, Evidence for glucose-mediated covalent cross-linking of collagen after glycosylation *in vitro*, *Biochem. J.* 225 (1985) 745–752.
- [18] T.J. Sims, N.C. Avery, A.J. Bailey, Quantitative determination of collagen crosslinks, *Methods Mol. Biol.* 139 (2000) 11–26.
- [19] F.A. Shamsi, A. Partal, C. Sady, M.A. Glomb, R.H. Nagaraj, Immunological evidence for methylglyoxal-derived modifications *in vivo*. Determination of antigenic epitopes, *J. Biol. Chem.* 273 (1998) 6928–6936.
- [20] M. Bendayan, Immunocytochemical detection of advanced glycated end products in rat renal tissue as a function of age and diabetes, *Kidney Int.* 54 (1998) 438–447.
- [21] K. Mikulíková, A. Eckhardt, J. Kunes, J. Zicha, I. Miksik, Advanced glycation end-product pentosidine accumulates in various tissues of rats with high fructose intake, *Physiol. Res.* 57 (2008) 89–94.
- [22] F.S. Parker, Applications of Infrared, Raman and Resonance Raman Spectroscopy in Biochemistry, Plenum Press, New York, 1983.
- [23] N. Mainreck, S. Brézillon, G.D. Sockalingum, F.X. Maquart, M. Manfait, Y. Wegrowski, Rapid characterization of glycosaminoglycans using a combined approach by infrared and Raman microspectroscopies, *J. Pharm. Sci.* 100 (2011) 441–450.
- [24] R. Roy, A. Boskey, L.J. Bonassar, Processing of type I collagen gels using nonenzymatic glycation, *J. Biomed. Mater. Res. A* 93 (2010) 843–851.
- [25] E. Millerot-Serruot, M. Guilbert, N. Fourné, W. Witkowski, G. Said, L. Van Gulick, C. Terryn, J.M. Zahm, R. Garnotel, P. Jeannesson, 3D collagen type I matrix inhibits the antimigratory effect of doxorubicin, *Cancer Cell Int.* 13 (2010) 10–26.
- [26] C. Petitbois, G. Gouspillou, K. Wehbe, J.P. Delage, G. Déleris, Analysis of type I and IV collagens by FT-IR spectroscopy and imaging for a molecular investigation of skeletal muscle connective tissue, *Anal. Bioanal. Chem.* 386 (2006) 1961–1966.
- [27] S. Jaisson, S. Lorimier, S. Ricard-Blum, G.D. Sockalingum, C. Delevallée-Forte, G. Kegelaer, M. Manfait, R. Garnotel, P. Gilleri, Impact of carbamylation on type I collagen conformational structure and its ability to activate human polymorphonuclear neutrophils, *Chem. Biol.* 13 (2006) 149–159.
- [28] R.J. Clark, P.M. McDonough, E. Swanson, S.U. Trost, M. Suzuki, M. Fukuda, W.H. Dillmann, Diabetes and the accompanying hyperglycemia impairs cardiomyocyte calcium cycling through increased nuclear O-GlcNAcylation, *J. Biol. Chem.* 278 (2003) 44230–44237.
- [29] S.V. Pizzo, M.A. Lehrman, M.J. Imber, C.E. Guthrow, The clearance of glycoproteins in diabetic mice, *Biochem. Biophys. Res. Commun.* 101 (1981) 704–708.

- [30] A.K. Death, E.J. Fisher, K.C. McGrath, D.K. Yue, High glucose alters matrix metalloproteinase expression in two key vascular cells: potential impact on atherosclerosis in diabetes, *Atherosclerosis* 168 (2003) 263–269.
- [31] R. Meerwaldt, T. Links, C. Zeebregts, R. Tio, J.L. Hillebrands, A. Smit, The clinical relevance of assessing advanced glycation endproducts accumulation in diabetes, *Cardiovasc. Diabetol.* 7 (2008) 29.
- [32] A. Lapolla, A. Mosca, D. Fedele, The general use of glycated haemoglobin for the diagnosis of diabetes and other categories of glucose intolerance: still a long way to go, *Nutr. Metab. Cardiovasc. Dis.* 21 (2011) 467–475.
- [33] A.G. Markelz, A. Roitberg, E.J. Heilweil, Pulsed terahertz spectroscopy of DNA, bovine serum albumin and collagen between 0.1 and 2.0 THz, *Chem. Phys. Lett.* 320 (2000) 42–48.
- [34] M. Nassa, P. Anand, A. Jain, A. Chhabra, A. Jaiswal, U. Malhotra, V. Rani, Analysis of human collagen sequences, *Bioinformation* 8 (2012) 26–33.
- [35] R. Usha, S.M. Jaimohan, A. Rajaram, A.B. Mandal, Aggregation and self assembly of non-enzymatic glycation of collagen in the presence of amino guanidine and aspirin: an in vitro study, *Int. J. Biol. Macromol.* 47 (2010) 402–409.
- [36] A. Travo, O. Piot, R. Wolthuis, C. Gobinet, M. Manfait, J. Bara, M.E. Forgue-Lafitte, P. Jeannesson, IR spectral imaging of secreted mucus: a promising new tool for the histopathological recognition of human colonic adenocarcinomas, *Histopathology* 56 (2010) 921–931.
- [37] K. Belbachir, R. Noreen, G. Gouspillou, C. Petibois, Collagen types analysis and differentiation by FTIR spectroscopy, *Anal. Bioanal. Chem.* 395 (2009) 829–837.